Computational Engineering and Physical Modeling 2-2 (2019) 49-61

Contents lists available at **CEPM**

Computational Engineering and Physical Modeling

Journal homepage: www.jcepm.com

Time-Frequency Localization of Earthquake Record by Continuous Wavelet Transforms

Kh. Keyani[1], J. Raeisi[2,3], A. Heidari[2*]

1. Department of Civil Engineering, Islamic Azad University Shahrekord Branch, Shahrekord, Iran
2. Department of Civil Engineering, Shahrekord University, Shahrekord, Iran
3. Researcher, Charmahal and Bakhtiari Water and Wastewater Company, Ministry of Energy, Iran

Corresponding author: *heidari@eng.sku.ac.ir*

https://doi.org/10.22115/CEPM.2019.193015.1065

ARTICLE INFO

Article history:
Received: 06 July 2019
Revised: 12 November 2019
Accepted: 13 November 2019

Keywords:
Earthquake record;
Time-frequency;
Localization;
Time series;
Continuous wavelet transform.

ABSTRACT

Wavelet analysis is a new mathematical method and has been increasingly applied in engineering in recent years. Unlike Fourier transform, this method is particularly appropriate for non-stationary processes. Exceptional localization can be allowed using wavelet transform, both in time and frequency domains. Wavelet transform has been rarely used in earthquake engineering. A preliminary study of continuous wavelet transforms (CWTs) was conducted in this paper. As a rather novel technique, CWT application has generated enormous interest in recent years. It has been successfully employed in many fields, including the theories of communication and ordinary, partial differential equations, signal and image processing, and numerical analysis. As evidenced, exceptional localizations of time-frequency domains have become possible through CWTs. In this paper, CWT capability of providing a full time-frequency representation of an earthquake record was demonstrated. The Morlet mother wavelet was utilized to calculate the time-frequency localization of the desired earthquake records. In this method, the time series of the earthquake records, which were broken in a wave flume, demonstrated the ability of the wavelet transform technique in detecting the complex variabilities of signals in the time-frequency domain. In this investigation, various spectral representations resulting from the CWTs were discussed and their applications for earthquake records were shown.

How to cite this article: Kiyani K, Raeisi J, Heidari A. Time-Frequency Localization of Earthquake Record by Continuous Wavelet Transforms. Comput Eng Phys Model 2019;2(2):49–61. https://doi.org/10.22115/cepm.2019.193015.1065

1. Introduction

Wavelet analysis is particularly suitable for non-stationary processes and can yield localized time-frequency information that cannot be available through the traditional Fourier transform (FT). Wavelet transform, is used an advanced tool in processing signal. Wavelet abilities have been used in different fields of civil engineering such as water engineering, structure engineering and soil engineering [1–3]. Also there are many researches about the application of wavelet transform in earthquake engineering [4–11]. A signal can be expressed in terms of sum of a series of sinus and cosines using Fourier transform (FT) and fast Fourier transforms (FFT). However: it has only frequency resolution and no time resolution in the FT and FFT methods [12,13]. Another disadvantage of the FT is that low and high frequencies of signal can't be separated by this method [14]. One solution for overcoming the shortcomings of the FT is application of wavelet transform (WT) [15]. In this method, a fully scalable window can be used for solving the signal-cutting problem. The window is moved along the signal and the spectrum is determined for every position.

WT application in earthquake engineering has been investigated in numerous studies. For example, Alonso et al. [16] used orthogonal WTs for identifying the stiffness loss in a spring-mass-damper system with a single degree of freedom. A quantitative approach was adopted by Yaghmaei-Sabegh [17] to detect pulse-like ground motions based on CWT. this approach is able to clearly identify sudden jumps in the time history of earthquake records by considering the contributions of different frequency levels. Nagarajaiah and Basu [18] developed a short-time Fourier transform (STFT), empirical mode decomposition, wavelet techniques and Hilbert transform (HT) for decomposing the free vibration responses of multi degree of freedom systems into their modal components. When the modal components were gained, each one was processed using HT to find the modal frequency and damping ratios. Pioldi and Rizzi [19] developed modal identifications of output-only structural systems through a refined frequency domain decomposition approach. The identification method was combined with a Gabor wavelet transform, which resulted in an effective and self-contained outline of time-frequency analysis. Ansari et al [20] examined the characteristics and capabilities of a wavelet denoising method for correcting highly noisy earthquake records. In the frequency domain, this technique was found to be able to attenuate noises in the whole frequency range of engineering, whereas in the time domain, it could detect and eliminate noises. Also, some research has been conducted on the use of WT for earthquake records. Todorovska et al predicted the goodness-of-fit of strong ground motions from earthquakes through the wavelet approximations of nonlinear structural responses and concluded that strong motion records on a wavelet basis can be developed and represented as the sum of pulses with a relatively small number [21]. Pnevmatikos and Hatzigeorgiou [22]described the application of discrete wavelet transform (DWT) for the damage detection of a framed structure subjected to strong earthquake excitations and the results revealed the effectiveness of this approach. Also, Heidari et al did a lot of research on wavelets and their applications [23,24]. They used types of DWT for dynamic analysis of structures induced by earthquake loads [25,26]. Then they optimized the structures [27,28] and approximated their strong ground motions [29]. Also, many researches have been conducted about the effect of earthquake on buildings [30,31].

In this article, CWT application for processing earthquake records was discussed and an attempt was made to present some beneficial quantitative results. The research was organized as follows: An overview of FT was given in the 2nd section. A discussion on the STFT theory and its resolution was provided in the 3rd section. WT fundamentals and its difference from FT were presented in the 4th section. Section 5 was dedicated to CWT application for processing earthquake records and finally, the main conclusions were given in section 6.

2. Fourier transform

A function of time (a signal) is decomposed into its constituent frequencies by the Fourier transform (FT). This process is similar to the way can be expression of a musical chord based on the volumes and frequencies of its constituent notes. The term Fourier transform denotes to both the frequency domain representation and the mathematical operation, relating the frequency domain representation with a function of time. The Fourier transform of a function of time is a complex-valued function of frequency. In this function magnitude (modulus) shows the value of frequency in the original function. Also; the argument of FT is the phase offset of the basic sinusoid in that frequency. The Fourier transform is not restricted to functions of time, while the domain of original function is called "time domain". The original function can be synthesized from its frequency domain representation by a transform namely inverse Fourier transform.

If a signal s*(t)* fulfills the finite energy (E) condition, it will be defined as follow [32]:

$$E = \int_{-\infty}^{+\infty} |s(t)|^2 dt < \infty \tag{1}$$

Then, the FT of *s(t)* exists as follows [32]:

$$S(f) = \int_{-\infty}^{+\infty} s(t) e^{-2\pi f t i} dt \tag{2}$$

where *t* and *f* indicate time and frequency, respectively. A capital letter *S* is used to represent the FT of *s*. The inverse FT is displayed as follows [32]:

$$s(t) = \int_{-\infty}^{+\infty} S(f) e^{2\pi f t i} df \tag{3}$$

Let's assume a fixed random procedure for signal s*(t)*. Unlike the deterministic signal of the finite energy, an unrestrained total energy will be achieved. Via the frequency distribution of the signal power, *E*/*T*, we can overcome this problem. As *T* represents the record time series, the function of *E*/*T* quantity will be time-restricted.

2.1. Short time fourier transforms

The short-time Fourier transform (STFT), is a Fourier-related transform used to determine the sinusoidal frequency and phase content of local sections of a signal as it changes over time [33].

To produce a stationary signal *s(t)* for inserting time information into its frequency domain, dividing the signal into sufficiently small segments would be an obvious alternative. Then, FT can be applied to each segment. To this goal, the boxcar window as a frequently used window function *w* is selected in the form of the following unsmoothed Gaussian function [34]:

$$w(t) = e^{(\frac{t}{\sqrt{2a}})^2} \tag{4}$$

The window width is determined by a. Through the multiplication of the window function by the signal, another signal is produced. This method is known as STFT.

Let's assume T0 to be the window width. Then, by regarding the time instant t0, the time intervals of t0-T0/2 and t0+T0/2 are overlapped by the window function. STFT for time t0 can be provided by multiplying signal s(t) by window w and integrating the product within this interval. Then, the window is shifted to a new position via the time step *Δt* until the signal stops. A summary of the whole process of STFT determination is presented as follows [34]:

$$STFT(\tau, f) = \int_t s(t)w^*(t - \tau)e^{-2\pi fti}dt \tag{5}$$

where a complex conjugate quantity is represented by the asterisk. The time-frequency transformation of the signal can be found through a new STFT coefficient calculation for every time τ and frequency *f*.

Despite FT, the window in STFT has a limited length and thus, no perfect resolution of the frequency can be achieved. This perfect resolution can be obtained by assuming an unlimited length of the window, but at the cost time of a complete information loss. Thus, an adequately short window should be chosen for gaining a stationary record. By making the window narrower, a better time resolution will be achieved; however, a worse resolution of frequency will be inevitable. Besides being applied to the positions and momentums of moving particles in quantum mechanics, this principle can be utilized to get the time-frequency information of a signal. The types of spectral components existing in their related time instances are not known. A poor frequency, but good time resolution can be represented by a narrow window and vice versa. It should be noted that the stationary state may be violated by a wide window. The resolution dilemma in the time-frequency domain can be somewhat solved by wavelet transform.

3. Wavelet transform

Wavelet transform is used in the variation analysis of time series [19]. FT does not refer to a frequency location. Time localization can be obtained using STFT. Also, window length has been regarded to be fixed. Unlike FT, WT considers the length of an analyzer window in relation with frequency. This transform changes the time series into a 3D space, including time, scale, and magnitude][1][1. enerally, the CWT of signal s*(t)* is defined as follows [35]:

$$CWT(\tau, b) = \int_{-\infty}^{\infty} s(t)g^*(\tau, b)dt \tag{6}$$

where $g(.)$ is the mother wavelet; variable $\tau > 0$ denotes the scale factor; b indicates wavelet translation over time; and $CWT(\tau, b)$ represents wavelet coefficient, which is obtained by applying the transform on the time series *s(t)* in a scale τ based on a time delay *b*. All the window functions are called daughter wavelets that can be calculated as follows [35]::

$$g(\tau,b)=\frac{1}{\sqrt{b}}g(\frac{t-\tau}{b}) \quad (7)$$

3.1 Continuous wavelet transform

The wavelet at a given scale corresponding to a frequency is close to a signal, which includes a major component of that frequency at a particular location. At this point, the corresponding coefficient of $CWT(\tau,b)$ possesses a rather large value. Hence, the $CWT(\tau,b)$ is regarded as a microscope characterized by magnification b^{-1}, a location determined by parameter τ, and the optics specified by function $g(\tau,b)$. The simplest method to be adopted is to determine $CWT(\tau,b)$ via integral Equation 6, but it is the most time-consuming approach. Alternatively, the spectral $CWT(\tau,b)$ can be represented as [36]:

$$WT(\tau,b)=\sqrt{b}\int_{-\infty}^{+\infty}e^{\tau\omega i}G^{*}(b\omega)S(\omega)d\omega \quad (8)$$

where $G(\omega)$ and $S(\omega)$ stand for the FT of $g(t)$ and $s(t)$, respectively.

The types of features present in the time series are commonly reflected by the CWT. A boxcar-like wavelet and a smooth function are more suitable for the time series of sharp steps and the smoothly varying ones, respectively. However, it will not be critical to choose a wavelet function if the spectra of the wavelet power are not primarily focused on. Morlet wavelet is a widely utilized mother wavelet that can be exhibited as follows [37]:

$$g(t)=\mathrm{e}^{-\left(\frac{t}{\sqrt{2}}\right)^{2}}\mathrm{e}^{\mathrm{ict}} \quad (9)$$

Using Equation 7, Morlet wavelet takes the following form [37]:

$$g(\tau,b)=\frac{1}{\sqrt{b}}\mathrm{e}^{-\left(\frac{t-\tau}{\sqrt{2}b}\right)^{2}}\mathrm{e}^{ic\frac{t-\tau}{b}} \quad (10)$$

A clear representation of the frequency nature of parameter c is achieved by assuming $c=2\pi$. Then, Equation 10 can be displayed as follows:

$$g(\tau,b)=\frac{1}{\sqrt{b}}\mathrm{e}^{-\left(\frac{t-\tau}{\sqrt{2}b}\right)^{2}}\mathrm{e}^{2\pi i\frac{t-\tau}{b}} \quad (11)$$

The sinusoidal wave of the frequency of $\frac{2\pi}{b}$; should represented by $\mathrm{e}^{2\pi i\frac{t-\tau}{b}}$ to treat the scale dilation b as a period. To make a more complete picture of a wavelet function, using a set of scales b in Equation 11 would be necessary. It is easy to take this set of scales as a function of powers-of-two coefficients [38]:

$$b_i=b_0 2^{i\delta} \qquad i=1,2,\dots.M \quad (12)$$

in which

$$M=\frac{1}{\delta}log_2(N\Delta t b_0^{-1}) \quad (13)$$

where N and Δt are the number of values in the time series and time sampling, respectively. b_0 and b_M represent the smallest and largest reasonable scales, respectively. To obtain an approximate $2\Delta t$ for the equivalent Fourier period, a proper value of b_0 should be selected. To provide sufficient sampling in scale b, δ as a representative of a scale factor should be considered. A value of nearly *0.5* for δ in Morlet wavelet would be still the largest value depicting a smooth wavelet spectrum. Nonetheless, finer resolutions are resulted by the smaller values of δ. Similar to STFT, in which a signal is multiplied by a window, WT analysis is performed using a wavelet. However, the width of the window changes by computing the transform for each spectral component, which is the most important feature of WT. To examine some properties of WT energy, it is first shown to conserve the total energy as follows:

$$\int_{-\infty}^{+\infty} |s(t)|^2 dt = \frac{1}{c_\psi} \int_0^{\infty} \int_0^{+\infty} \frac{|WT(\tau,b)|^2}{b^2} d\tau db \tag{14}$$

in which coefficient C_ψ is:

$$C_\psi^{-1} = \int_{-\infty}^{+\infty} \frac{|G(\omega)|^2}{\omega} \, d\omega \tag{15}$$

Where *G(ω)* represents the FT of function *g(t)*. Using the wavelet transform and coefficientC_ψ, various wavelet energy spectra and spectral densities can be defined. Specially, the so-called time-scale energy density can be determined as follows:

$$E_1 = |WT(\tau,b)|^2 b \tag{16}$$

Using the integration of scale b into Equation 16, the local energy density can be calculated as [39]:

$$E_2 = \frac{1}{c_\psi} \int_0^{\infty} E_1 b^{-1} db \tag{17}$$

The global wavelet energy spectrum E_3 can be obtained by integrating time τ into Equation 16 :

$$E_3 = \int_0^{\infty} E_1 dt \tag{18}$$

Torrence and Compo developed a reduced amount of the necessary smoothing with an increasing scale to make the smoothed Fourier spectrum approach [38]. Percival also indicated the global wavelet spectrum[40]. The total energy of time series *s(t)* can be determined as follows:

$$E = \frac{1}{c_\psi} \int_0^{\infty} E_3 b^{-1} db \tag{19}$$

By substituting Equations 16 and 18 into Equation 19, we will get the following equation:

$$E = \frac{1}{c_\psi} \int_0^{\infty} \int_{-\infty}^{+\infty} E_1 b^{-1} d\tau db = \frac{1}{c_\psi} \int_0^{\infty} \int_{-\infty}^{+\infty} |WT(\tau,b)|^2 b^{-2} d\tau db \tag{20}$$

This would verify the conservation of energy represented in Equation 14.

4. Resemblance of wavelets to fourier modes

In this section, the association between WT and FT will be presented for interpreting the processing results of earthquake records. This is not a direct relationship for arbitrary wavelets. However, the relation between WT and FT in Morlet wavelet was presented owing to its periodic feature in this paper. Assuming the periodic wave of frequency ω_0 and unit amplitude of

$$s(t) = e^{\omega_0 t} \tag{21}$$

As shown, the FT of the signal is $S(\omega)=\delta(\omega-\omega_0)$, in which δ stands for Dirac's delta function. Through Equation 8, we get:

$$WT(\tau, b) = \sqrt{b} \int_{-\infty}^{+\infty} e^{\omega\tau i}\, G^{*(b\omega)\delta(\omega-\omega_0)d\omega} = \sqrt{b}\, e\text{^}(\omega\_0\, \tau i)\, G\text{^} *\ (b\omega\_0\,) \tag{22}$$

Thus,

$$|WT(\tau, b)|^2 = b|G^*(b\omega_0)|^2 \tag{23}$$

Regarding Equation 9, Fourier transform $G^*(b\omega_0)$ in Morlet wavelet will be as follows:

$$|G^*(b\omega_0)| = e^{-(b\omega_0 - c)} \tag{24}$$

By substituting Equation 24 into Equation 23, we get the following condition:

$$|WT(\tau, b)|^2 = be^{-(b\omega_0 - c)^2} \tag{25}$$

Thereby, a maximum correlation is achieved between the WT and a component of FT with frequency ω_0, as follows:

$$\frac{\partial[|\mathrm{WT}(\tau,\mathrm{b})|^2]}{\partial \mathrm{b}} = 0 \tag{26}$$

or

$$2\omega_0^2 b^2 - 2c\omega_0 b - 1 = 0 \tag{27}$$

Equation 27 can be realistically solved only by the following equation:

$$b = (2\omega_0)^{-1}(c + \sqrt{c^2 + 2}\,) \tag{28}$$

Considering $\omega_0 = 2\pi T_0^{-1}$, a linear relationship is yielded between scale b and period T_0 in the following form:

$$b = (4\pi)^{-1}(c + \sqrt{c^2 + 2}\,)T_0 \\ = \alpha\, T_0 \tag{29}$$

where

$$\alpha = (4\pi)^{-1}(c + \sqrt{c^2 + 2}\,) \tag{30}$$

Equation 29 represents scale b as a physical dimension for time. Equation 30 results in $\alpha = 1.0125$ by assuming $c = 2\pi$. When $c = 2\pi - (4\pi)^{-1} \cong 6.2036$, scale b becomes completely equivalent to T_0 ($\alpha = 1$). The value of c=6.2036 was applied in this paper as discussed below. The second term of Morlet wavelet representing an oscillatory nature is underlined by this value, which is a very suitable choice for processing the data of earthquake waves [41]. Thus, almost identical values are obtained for scale b and Fourier period T in Morlet wavelet. Notably, Fourier period would be differerent from scale b in other mother wavelets. For instance, Fourier period T would be 4 times larger than scale b for Mexican hat wavelets.

5. Results and discussion

5.1. CWT Application to earthquake records

In this section, 2 examples of CWT application for processing earthquake records, i.e., Bam (2003) and Silakhor (2006) earthquakes in Iran will be presented and the records will be decomposed with a time interval of 0.02 s.

Bam earthquake happened at 01:56:56 GMT around Bam city in southeastern Iran at the local time of 05:26:26 A.M on the 26th of December 2003 (Mw=6.5) and led to a great life loss since most of the inhabitants were sleeping then.

Silakhor earthquake of March, 31, 2006 (Mw=6.1) occurred around Dorod city in western Iran at 02:40:04 GMT (local time of 04:47:00). Here, the FT and CWT of Silakhor earthquake were computed. Its earthquake record and FT are exhibited in Figures 4 and 5, respectively.

5.1. Example 1: bam earthquake record

Here, a computation of the FT and CWT of Bam earthquake were presented. The earthquake record and FT are displayed in Figures 1 and 2, respectively. The CWT of the earthquake record is portrayed in Figure 3. By comparing Figures 2 and 3, the highest frequency of the earthquake record was found to be 0.69 Hz corresponding to scale 1.48. The major part of FT demonstrated a frequency range of 0.6-0.75 Hz, which was similar to the scale range of 1.35-1.68, thus indicating the highest range of frequency. The time of each frequency could be distinguished by referring to Figure 3 and the output measurements programmed for this purpose. For instance, the time for the frequency of 0.69 Hz corresponding to scale 1.48 is 18.28 sec. The time range of the above-mentioned frequency range was 18.22-18.4 sec, during which all the constructions with the same frequencies as the dominant frequency of Bam earthquake (0.69 Hz) could have been most dangerously affected. Similarly, the time ranges of the other frequencies of the earthquake record could be computed.

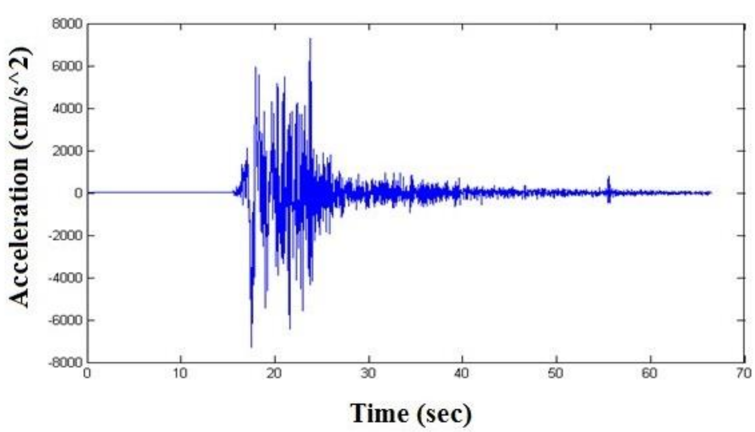

Fig. 1. The Bam earthquake record.

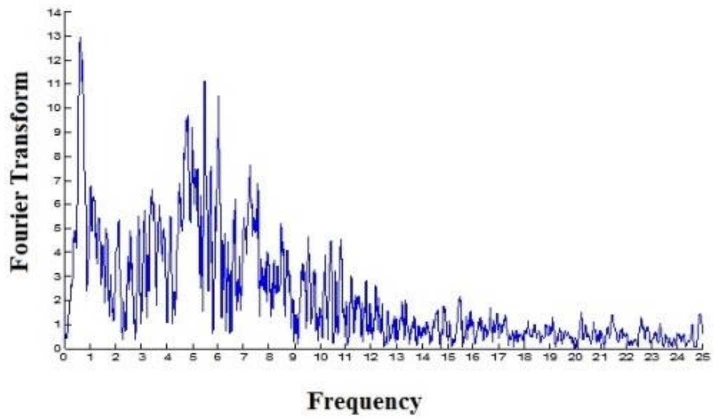

Fig. 2. FT of the Bam earthquake record.

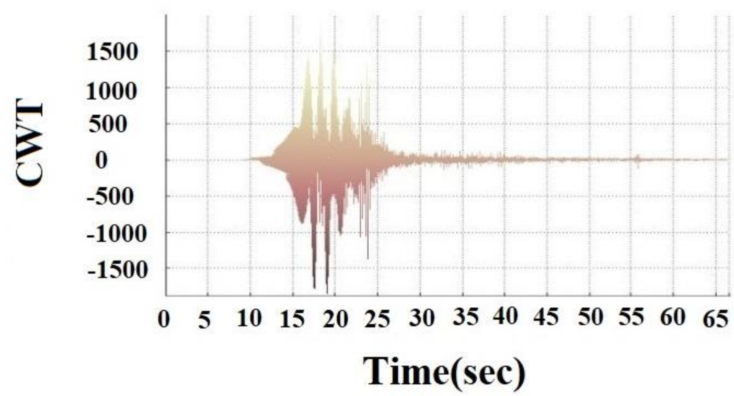

Fig. 3. Two dimensional WT of the Bam earthquake record.

Example 2: Silakhor earthquake record

The CWT of the earthquake record is portrayed in Figure 6. By comparing Figures 5 and 6, the highest frequency of the earthquake record was discovered to be 3.58 Hz corresponding to scale 0.28. The major part of FT had a frequency range of 3.3-4.3 Hz, representing the highest frequency range. This range of frequency could be attributable to the scale range of 0.23-0.3. By referring to Figure 6 and the output measurements programmed, we were able to distinguish the time of each frequency. For instance, the time of the frequency 3.58 Hz corresponding to scale 0.28 was found to be 25.5 sec. Accordingly, the time range of the above-mentioned frequency range was 25-26 sec, indicating the most perilous range for all the constructions that had a frequency similar to the dominant frequency of the earthquake record. The main frequency of Silakhor earthquake was found to be 3.58 Hz. Similarly, we could compute the times of the other frequencies for this earthquake record.

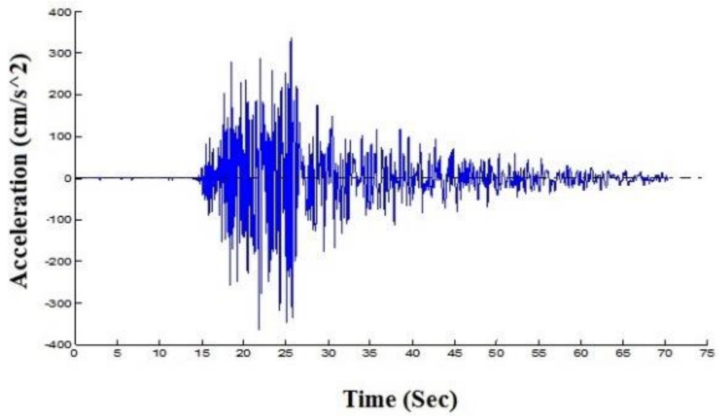

Fig. 4. The Silakhor earthquake record.

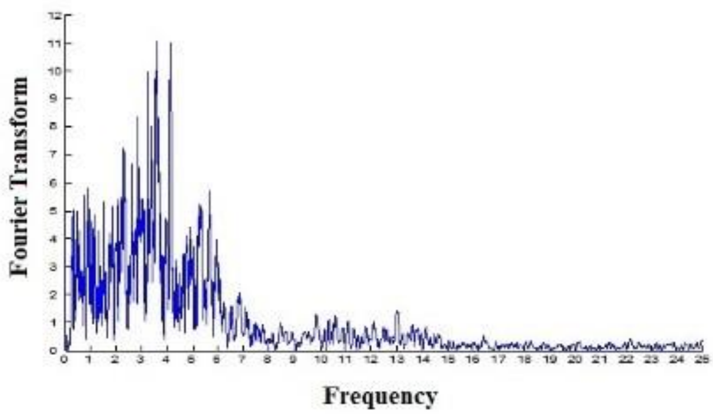

Fig. 5. FT of the Silakhor earthquake record.

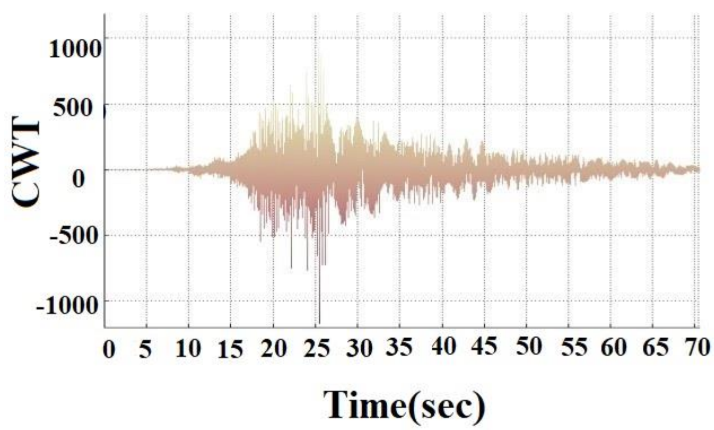

Fig. 6. Two dimensional WT of the Silakhor earthquake record.

6. Conclusion

CWT allows localization both in the time domain and in the frequency domain, which can be changed from a minimum to a maximum value as chosen by the user. The two mentioned examples demonstrated CWT capability in providing a full time-frequency localization of earthquake records. The processing of the time series recorded for Bam and Silakhor earthquakes revealed CWT ability in detecting the complex variations of the relevant signals within the time-frequency domains. The changes in the frequencies corresponding to maximum WTs at particular times highly resembled those occurred in the recorded frequencies. Interestingly, the impacts of some low-frequency components that cannot be clearly depicted by classical spectrum can be represented by WT. Besides these results, some other resuls are also obtained as following:`

- If the time of frequencies is given, the second related to the most motivation of structure can be obtained using structural dynamic methods.
- After specifying frequency time, if Resonance phenomenon is possible, the time related to resonance frequency can be obtained.
- After specifying frequency time, if the active control systems of structure is available, the system can be made smart that in those seconds, they will make better performance for the structure.

References

[1] Lafrenière M, Sharp M. Wavelet analysis of inter-annual variability in the runoff regimes of glacial and nival stream catchments, BowLake, Alberta. Hydrol Process 2003;17:1093–118. doi:10.1002/hyp.1187.

[2] Naga P, Eatherton MR. Analyzing the effect of moving resonance on seismic response of structures using wavelet transforms. Earthq Eng Struct Dyn 2014;43:759–68. doi:10.1002/eqe.2370.

[3] Smyrou E, Bal İE, Tasiopoulou P, Gazetas G. Wavelet analysis for relating soil amplification and liquefaction effects with seismic performance of precast structures. Earthq Eng Struct Dyn 2016;45:1169–83. doi:10.1002/eqe.2701.

[4] Yaghmaei-Sabegh S. Wavelet-based analysis for pulse period of earthquake ground-motions 2013.

[5] Gholizadeh S, Samavati OA. Structural optimization by wavelet transforms and neural networks. Appl Math Model 2011;35:915–29.

[6] Kaveh A, Mahdavi VR. A new method for modification of ground motions using wavelet transform and enhanced colliding bodies optimization. Appl Soft Comput 2016;47:357–69.

[7] Sharbati R, Khoshnoudian F, Ramazi HR, Amindavar HR. Stochastic modeling and simulation of ground motions using complex discrete wavelet transform and Gaussian mixture model. Soil Dyn Earthq Eng 2018;114:267–80. doi:10.1016/j.soildyn.2018.07.003.

[8] Huang D, Wang G. Energy-compatible and spectrum-compatible (ECSC) ground motion simulation using wavelet packets. Earthq Eng Struct Dyn 2017;46:1855–73. doi:10.1002/eqe.2887.

[9] Heidari A, Raeisi J, Kamgar R. The application of wavelet theory with denoising to estimate the parameters of earthquake. Sci Iran 2019:0–0. doi:10.24200/sci.2019.50675.1815.

[10] Raeisi J. Investigation of strong ground motion using a wavelet theory for hydraulic structure in far fault. MSc Thesis, Department of Civil Engineering, Shahrekord University, Iran. Shahrekord, Iran. 2017.

[11] Heidari A, Raeisi J. A new method for calculating earthquake characteristics and nonlinear spectra using wavelet theory. J Rehabil Civ Eng 2020;8:50–62.

[12] R. P. The Wavelet Tutorial, http://www.public.iastate.edu/~rpolikar/WAVELETS/ wave letindex html 1996.

[13] Chen W-K. The circuits and filters handbook. CRC Press; 2002.

[14] Strang G, Nguyen T. Wavelets and filter banks. SIAM; 1996.

[15] J.B.T.M. R. Wavelets for Signal and Image Processing. Lecture notes, Department of Computing Science, Rijksuniversiteit Groningen, NL 1993.

[16] Alonso RJ, Noori M, Saadat S, Masuda A, Hou Z. Effects of excitation frequency on detection accuracy of orthogonal wavelet decomposition for structural health monitoring. Earthq Eng Eng Vib 2004;3:101–6.

[17] Yaghmaei-Sabegh S. Detection of pulse-like ground motions based on continues wavelet transform. J Seismol 2010;14:715–26.

[18] Nagarajaiah S, Basu B. Output only modal identification and structural damage detection using time frequency & wavelet techniques. Earthq Eng Eng Vib 2009;8:583–605. doi:10.1007/s11803-009-9120-6.

[19] Pioldi F, Rizzi E. A refined Frequency Domain Decomposition tool for structural modal monitoring in earthquake engineering. Earthq Eng Eng Vib 2017;16:627–48. doi:10.1007/s11803-017-0394-9.

[20] Ansari A, Noorzad A, Zafarani H, Vahidifard H. Correction of highly noisy strong motion records using a modified wavelet de-noising method. Soil Dyn Earthq Eng 2010;30:1168–81. doi:10.1016/j.soildyn.2010.04.025.

[21] Todorovska MI, Meidani H, Trifunac MD. Wavelet approximation of earthquake strong ground motion-goodness of fit for a database in terms of predicting nonlinear structural response. Soil Dyn Earthq Eng 2009;29:742–51. doi:10.1016/j.soildyn.2008.08.001.

[22] Pnevmatikos NG, Hatzigeorgiou GD. Damage detection of framed structures subjected to earthquake excitation using discrete wavelet analysis. Bull Earthq Eng 2017;15:227–48.

[23] Salajegheh E, Heidari A. Approximate dynamic analysis of structures for earthquake loading using FWT. Int J Eng 2007;20:37–47.

[24] Heidari A, Pahlavan sadegh S, Raeisi J. Investigating the Effect of Soil Type on Non-linear Response Spectrum Using Wavelet Theory. Int J Civ Eng 2019;17:1909–18. doi:10.1007/s40999-019-00394-6.

[25] Salajegheh E, HEYDARI A. Dynamic analysis of structures against earthquake by combined wavelet transform and fast Fourier transform 2002.

[26] Salajegheh E, Heidari A. Time history dynamic analysis of structures using filter banks and wavelet transforms. Comput Struct 2005;83:53–68. doi:10.1016/j.compstruc.2004.08.008.

[27] Salajegheh E, Heidari A. Optimum design of structures against earthquake by wavelet neural network and filter banks. Earthq Eng Struct Dyn 2005;34:67–82. doi:10.1002/eqe.417.

[28] Heidari A, Raeisi J. Optimum Design of Structures Against earthquake by Simulated Annealing Using Wavelet Transform. J Soft Comput Civ Eng 2018;2:23–33.

[29] Heidari A, Raeisi J, Kamgar R. Application of wavelet theory in determining of strong ground motion parameters. Iran Univ Sci Technol 2018;8:103–15.

[30] Bakhshi H, Khosravi H, Ghoddusi M. Evaluation of Seismic Behavior of Steel Shear Wall by Time History Analysis. Comput Eng Phys Model 2019;2:38–55.

doi:10.22115/cepm.2019.160278.1055.

[31] Torkian H, Keshavarz Z. Determining the drift in reinforced concrete building using ANFIS soft computing modeling. Comput Eng Phys Model 2018;1:1–11.

[32] Bracewell RN, Bracewell RN. The Fourier transform and its applications (Vol. 31999). New York: McGraw-Hill 1986.

[33] Sejdić E, Djurović I, Jiang J. Time–frequency feature representation using energy concentration: An overview of recent advances. Digit Signal Process 2009;19:153–83. doi:10.1016/j.dsp.2007.12.004.

[34] Griffin D, Lim J. Signal estimation from modified short-time Fourier transform. IEEE Trans Acoust 1984;32:236–43.

[35] Grossmann A, Kronland-Martinet R, Morlet. Reading and understanding continuous wavelet transforms. Wavelets Springer, Berlin, Heidelb 1990:2–20.

[36] Daubechies I. The wavelet transform, time-frequency localization and signal analysis. IEEE Trans Inf Theory 1990;36:961–1005. doi:10.1109/18.57199.

[37] Shyh-Jier Huang, Cheng-Tao Hsieh. High-impedance fault detection utilizing a Morlet wavelet transform approach. IEEE Trans Power Deliv 1999;14:1401–10. doi:10.1109/61.796234.

[38] Torrence C, Compo GP. A Practical Guide to Wavelet Analysis. Bull Am Meteorol Soc 1998;79:61–78. doi:10.1175/1520-0477(1998)079<0061:APGTWA>2.0.CO;2.

[39] Farge M. Wavelet transforms and their applications to turbulence. Annu Rev Fluid Mech 1992;24:395–458.

[40] PERCIVAL DP. On estimation of the wavelet variance. Biometrika 1995;82:619–31. doi:10.1093/biomet/82.3.619.

[41] Heidari A, Salajegheh E. Wavelet analysis for processing of earthquake records 2008.